LET Estimation of Heavy Ion Particles based on a Timepix-Based Si Detector

S Hoang[1], L Pinsky[2], R Vilalta[1] and J Jakubek[3]

[1] Department of Computer Science, University of Houston, USA
[2] Department of Physics, University of Houston, USA
[3] Department of Applied Physics and Technology, Czech Technical University in Prague, Czech Republic

E-mail: {smhoang,pinsky}@uh.edu, vilalta@cs.uh.edu, jan.jakubek@utef.cvut.cz

Abstract. Linear Energy Transfer (LET) is a measure of the energy transferred into a material as an ionizing particle passes through it. This quantity is useful in estimating the biological effects of ionizing radiation as expressed in dosimetric endpoints such as Dose-equivalent. Pixel detectors with silicon sensors --like the Medipix2 Collaboration's Timepix-based devices-- are ideal instruments to measure the total energy deposited by a transiting ionizing particle. In this paper we propose an approach for determining the amount of LET from track images obtained with a Timepix-based Si pixel detector. In particular, we have developed a method to calculate the angle of incidence for a heavy ion particle as it passes through a 300 μm thick Si sensor layer based on an analysis of the information in the cluster of pixel hits. Using that angle information, the path length traversed by the particle can be computed, which then facilitates estimating the degree of LET. Results from experiments with data taken at the HIMAC (Heavy Ion Medical Accelerator) facility in Chiba, Japan, and NASA Space Radiation Laboratory at Brookhaven in USA, demonstrate the effectiveness and resolution of our method to determine the angle of incidence and LET of heavy ion particles.

1. Introduction

One fundamental question in the search to develop a Space Radiation Dosimeter using the Timepix chip from the Medipix2 Collaboration is how Dose-equivalent can be extracted from the raw Timepix outputs. Dose is defined as the energy deposited by a source of radiation per unit mass of traversed matter. Dose-equivalent is the most common form to express the biological effects of the dose caused by a particular type of particle for radiation protection purposes. To calculate the Dose-equivalent, each type of potentially incident radiation is given a Quality Factor, also referred to as Relative Biological Effectiveness (RBE). As proposed by the National Council on Radiation Protection [NCRP 153 (2008)] regarding heavy ions in the space radiation environment, Quality Factor is a function of the LET of the traversing particle. LET is distinguishable from dE/dx (the kinetic energy lost by the primary ion per unit track length) in that it is a measure of the energy transferred to the local medium. LET_∞ is defined in a theoretical infinite medium, and should ultimately be equal to dE/dx. In a practical sense, however, the actual local LET is what physical detectors measure, and what really matters to assess risk to tissue in human exposure. As discussed below, one can reasonably infer the amount of LET in tissue based on a measurement in another medium such as silicon. The Timepix chip device has a 300 μm thick Si sensor with a volume of 6 x 10^{-2} cm^3 (2 cm^2 x 0.003 cm). Si has a density of d_{Si} = 2.3212, giving the Si detector layer a mass of ~0.14 g. Thus, one can determine the

Dose in Si in Gy, (D_{Si}), by multiplying the total absorbed energy in a TimePix detector by a single factor:

$$D_{Si} = E_{TimePix} \text{ (in KeV)} \{1 / [\, 0.14 \text{ g} \times 6.24 \times 10^{12} \text{ KeV/Gy g} \}$$
$$= E_{TimePix} \text{ (in KeV)} \{\, 1.153 \times 10^{-12} \,\} \text{ Gy} \quad (1)$$

In order to determine the Dose-equivalent, however, one needs to multiply the absorbed dose by a Quality Factor on a particle-by-particle basis. Since the Quality factor is a function of the LET (Figure 2), we need only determine the LET to achieve the value for the Dose-equivalent:

$$H = Q(LET) \,.\, D_{si} \text{ (Sv)} \quad (2)$$

Using the Timepix-based detector, LET can be measured from the total energy deposited (which is available from the calibrated Timepix chip) divided by the path length traversed by the particle as it passes through the Si layer. The thickness of the Si layer, which is 300 µm, can be used to calculate the total track length if it is possible to measure the track's angle of incidence, or its projected track length parallel to the surface of the detector. Note that for biological purposes, the dose in water or tissue is typically required, and a correction factor needs to be applied to convert the dose in Si into these other dose values. In practice, the conversion factor has a slight dependence on the velocity (or kinetic energy) of the particle depositing the dose, but that can be reasonably approximated by a single factor (~1.23) when the energy is not known. A study is in progress for determining the velocity of each individual particle from information contained in the combined pixel shape.

The raw Timepix output (Figure 1) is generated by the Medipix2 Timepix chip that is attached to an overlying Si sensor layer using the bump-bonding technique. The resulting detector is a hybrid semiconductor CMOS-based pixel detector made of 256 x 256 square pixels with the readout electronics for each pixel embedded within the footprint of each 55 µm square pixel. This device, developed by a collaboration based at CERN, is able to survive and perform for extended periods in strong radiation fields. When an incident charged particle penetrates the Si layer, it ionizes atoms along its path, producing a core of charge carriers that reflect the detail of the ionization along the track structures. These charges drift along and diffuse perpendicular to an applied bias-voltage field, which in turn causes the charge to be collected by the underlying pixels. The structures of the pixel clusters are complicated due both to the diffusion and to the existence of δ-rays, which are recoil electrons liberated by the ionization process. A careful analysis of these track structures (e.g., [1]) is needed to understand the behaviour of particles, such as their projected track length.

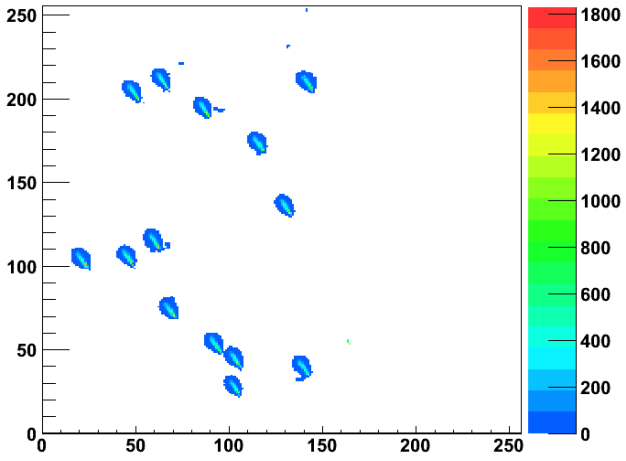

Figure 1. An output frame of Timepix

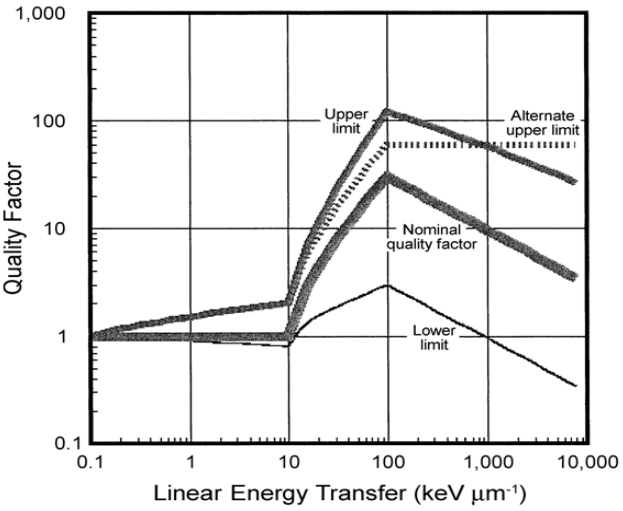

Figure 2. Quality Factor as a function of LET

For the particular analysis described in this paper, we employed the energy calibration method described in Section II below to obtain the total energy deposited in the Si sensor layer as a function of

the value read out from each individual pixel. Based on an analysis of the structure of the cluster of pixels for each track, we propose an algorithm for estimating angular resolution of incident charged particles. Given the raw Timepix output, we use a segmentation operator to identify clusters --groups of contiguous pixels forming track structures. We then apply a morphology operator to get the primary and stable shape of a cluster. By doing this, noise and δ-rays are effectively removed. The operator also helps to recognize and separate simple overlapping particles that occur when the exposure time is not short enough. A linear regression model has been found to determine the azimuthal direction of incidence. We extract track lengths based on an analysis of pixels projected onto this direction and perpendicular to it. The resolution of the angle of incidence is determined based on a formula which combines track lengths in these directions. Once one has the angle and the total energy, LET can be determined to consequently help us attain the Quality Factor and Dose-equivalent.

2. Energy calibration

We briefly describe the method developed by Jan Jakubek [4] to calibrate energy from the Timepix device to obtain the corresponding energy deposited on each pixel. By integrating the energy of all pixels belonging to a cluster, one can get the total energy deposited. The Time-Over-Threshold has been used for global operational mode in Timepix operation. In this mode, the integrated charge collected is measured by counting the number of Counter Clock pulses that occur while the output of the front-end charge sensitive preamp is above a default Threshold. As charge is collected at the input to the charge-sensitive preamp, the combined shaper circuit is set to produce a triangular-shaped pulse whose area and width are proportional to the charge collected. The leading edge of this pulse necessarily has an initial rise-time that introduces a simple nonlinearity for pulses very near the Threshold value. For pulses that significantly exceed the Threshold, the linearity of the effective ADC is excellent (as shown in Figure 3).

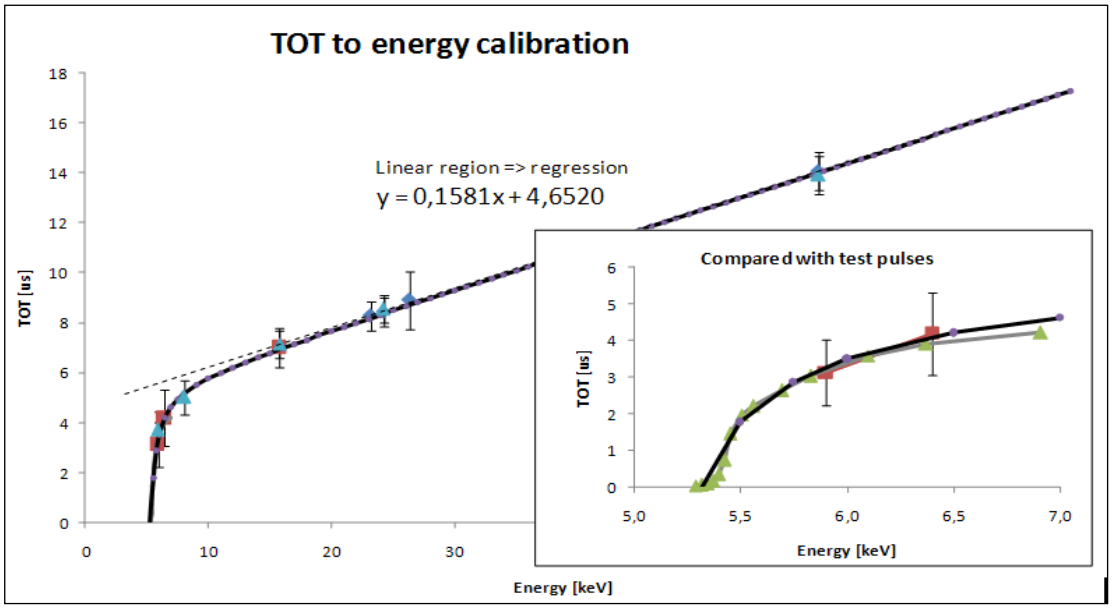

Figure 3. TOT to energy calibration

The shape of the curve in Figure 3 is caused by the rise time of the shaping circuit and the capacitance of the input stage. It is possible to fit this curve with a simple function:

$$TOT = a\,E + b - c/(E-t) \qquad (3)$$

where TOT is the recorded number of Counter-Clock pulses, E is the energy deposited in the detector that resulted in the charge collected by the pixel and a, b, c & t are the 4 parameters that need to be

determined for each pixel. Equation 3 can be inverted to yield the Energy as a function of the TOT value.

3. Incident angle estimation

When an energetic particle penetrates the detector layer, electrons and holes liberated along the particle's track drift in the electric field of the depletion bias voltage, diffusing both laterally and horizontally with respect to the field. The diffused charge will generally spread out over multiple pixels creating a cluster of pixels associated with a single event. This spreading follows an interesting pattern: the shape and energy intensity at pixels provide precise information about the azimuthal direction and the angle of incidence with respect to the normal direction. However, one cannot simply fit the shape with a certain model --such as an ellipse-- and determine the angle resolution based on the elongation. The existence of energetic δ-rays, the heightened recombination of electrons and holes in regions with very high levels of ionization (the so-called "plasma-effect") [6], and the effects of producing variations with different bias-voltage and source of charged particles [2][3], make the incident angle difficult to estimate accurately.

By looking carefully into the structure of clusters, we were able to identify three main components: a core part at the center of each cluster, the region immediately surrounding the core, called "skirt", and an δ-ray part which comes from recoil electrons liberated from the ionization process (Figure 4). The core contains most of the pixels with high energy, as it is the area where charges are collected from multiple overlapping electrons along the traversed path. The skirt contains low energy pixels, where electron densities are low. The core and the skirt part constitute the primary track or continent, the δ-ray part can be considered in the geographic analogy as peninsulas connecting to the continent. The δ-ray part also contains low energy levels that provide hints on the velocity or energy of the δ-rays in their length and total energy. The δ-rays begin deep within the core and emerge through the skirt, and they can be distinguished clearly if the energy of incident particle is high enough.

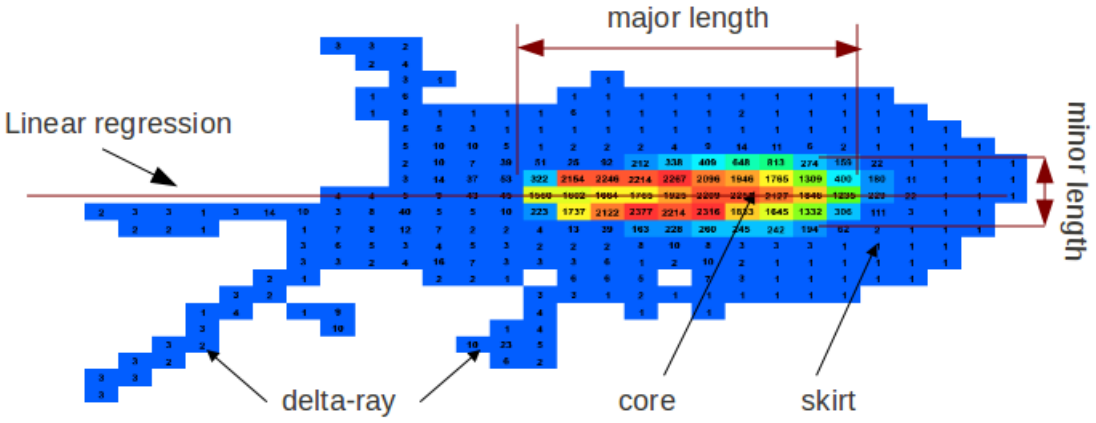

Figure 4. Cluster's components

The tails of δ-rays do not play an important role in calculating angle resolution, and were removed using a morphology operator. This operator iteratively removes low energy pixels with few neighbors. We determined an azimuthal direction of the track by employing a linear regression technique to fit a line over all remaining pixels that belong to the core and skirt parts. We applied this technique several times with different thresholds of energy and obtained an average to produce a slope that represents the "major direction" of the track. A "minor direction" can be easily obtained by finding a line perpendicular to this major direction. We projected all remaining pixels onto the major and minor directions and extracted two "track lengths". We then applied a formula that combines these two track lengths to obtain the proposed angle resolution. Note that using only *major* length for angular

estimation is not appropriate, as this length will vary considerably according to different applied bias-voltage and different unknown sources of particles.

To extract the effective track length on each direction, we divided the projected pixels into small and equal sections or bins, and accumulated the energy of pixels belonging to each bin. The number of bins is equal to the distance between the two farthest projected pixels. The result is a histogram in which the horizontal axis shows the bins, and the vertical axis shows the accumulated energy for each bin. Since the energy collection at each pixel and bin is a stochastic process, which means that in each individual case there is a degree of randomness in the cutoff point with respect to which bin belongs to the core part, which one belongs to the skirt part, and how much each bin contributes to the track length. For this reason, we applied a fuzzy set theory [7] to assign a membership function for the concept "core part". The membership value ranges from 0 to 1. For bins where the vertical value is above the mean of histogram, the membership value is 1. Otherwise, the membership value is defined as the ratio of the vertical value of each bin divided by the mean value for the entire histogram. The sum of all membership values is the length of the track for this direction.

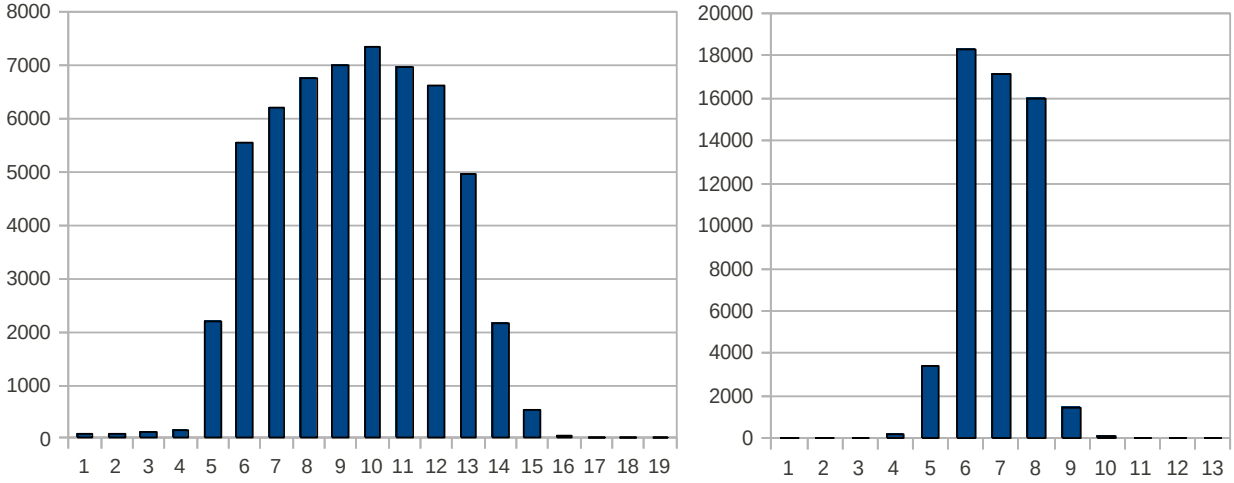

Figure 5. Energy histograms on the major direction (left) and the minor direction (right)

Figure 5 is an example of unmodified accumulated energy histograms for the cluster in Figure 4; the histogram corresponds to the major direction (Figure 5 left) and minor direction (Figure 5 right). In this case, the major direction has slope 0, parallel to the horizontal axis. One can see that the vertical values of bins that belong to the skirt part on the left and right hand side of the cluster are very small. As a result, their membership values contribute almost nothing to the track-lengths, no matter how many bins there are. A significant contribution comes from bins in the middle section, and the ones that are at the edge of this middle region are the only ones that need to be distinguished between the core and the skirt parts. Once the major and minor "track-length" have been determined, we propose the following formula to compute the incident angle.

$$\tan(\alpha) = \frac{55}{300}\left(major - \frac{minor - 1.5}{major + 1} minor \right) \quad (5)$$

In equation 5, 300 (μm) is the detector layer thick, 55 (μm) is the distance between two pixels. The other constants are assigned by finding a reasonable fit to data for the angles. However, equation 5 has shown to be accurate only for tracks whose angle of incidence passing through the sensor layer is more than 15 degrees with respect to the vertical. As such, we need a special initial algorithm to classify which tracks are likely to be vertical tracks from those which are most likely not. As the energy deposited of vertical tracks can be approximated by a two dimension normal distribution, likely vertical tracks can be distinguished by using the skewness to check whether the energy histogram

above is symmetric or not. We also compare the lengths of major and minor to check the equal diffusion in each direction. If the difference is very small, then the track is classified as a vertical track.

4. Experimental results

We use data taken at the HIMAC (Heavy Ion Medical Accelerator) facility in Chiba, Japan, and NASA Space Radiation Laboratory at Brookhaven in USA for our experiments. The data frames were taken at different angles and particle charges. In particular, we show experimental results for H-160MeV (0, 30, 45, 60 degree), He-180MeV (30, 45, 60 degree), He-100MeV (0, 30, 60, 75 degree), C-230MeV (0, 30, 45, 60, 85 degree), N-290MeV(0, 30, 60, 75 degree), O-230MeV (0, 20, 40, 60, 85 degree), Ne-600MeV (0, 20, 40, 60, 85 degree), Ar-290MeV (0, 30, 60, 85 degree), Ar-650MeV (0, 20, 40, 60, 85 degree), Fe-400MeV (0, 30, 60, 75, 85 degree). We typically analyzed one thousand frames that were taken such that each frame contains several clusters associated with corresponding events, but not enough to create a significant likelihood that the clusters will overlap. We evaluate the angles generated by our method and compare them to the true angles, which are generally known to a small fraction of a degree. Then we performed the analysis to determine the LET values for the tracks. The LETs generated from different angles are expected to be the same because the relatively small thickness of the sensor does not typically show a significant variation in the particles LET due to the reduction in the kinetic energy of the incident particle. These results demonstrate the resolution of our algorithm for determining the angle of incidence and LETs for these tracks.

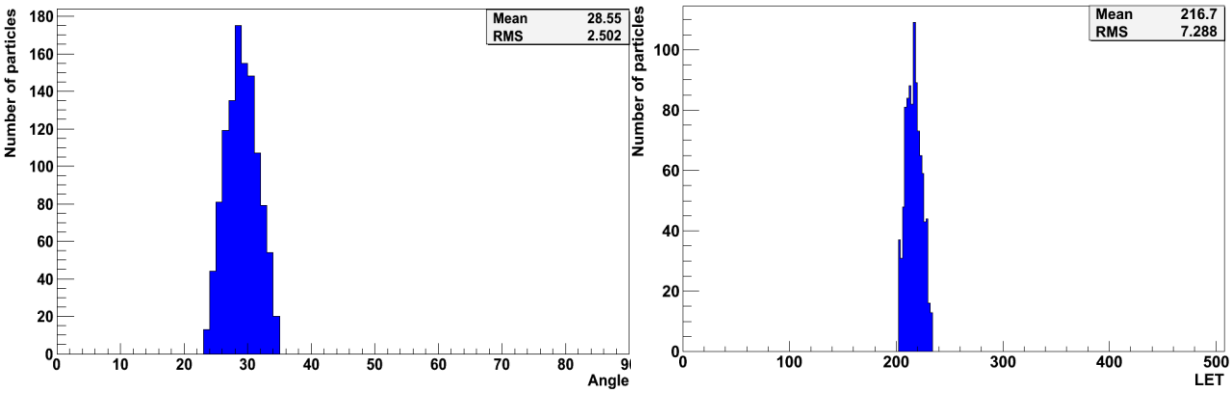

Figure 6. Angle and LET distribution at 30 degree of Fe-400MeV

Figure 6 is the angle and LET distributions of 30 degree of Fe-400MeV incidences, respectively. The results have the Gaussian distribution oscillating around a mean value with a standard deviation. The mean value is very close to the true angle and the standard deviation is small enough such that the error is acceptable. Table 1 shows the experimental angles and LETs compared to true ones for different angles and different ionizing particles. Cells in this table are left empty if data are not available. In fact, if LET is less than 10 then the resulting quality factor is approximately 1 (Figure 2). We define the LET by the total energy deposited (E) divided by the track length (L) of mass traversed matter, converted for tissue equivalent as described earlier. In our application, since L is always greater than 300μm (our sensor thickness), the quality factor will be approximately 1 if E is less than 3MeV. Therefore, we ignore clusters that have total energy deposited less than 3MeV and arbitrarily assign a quality factor of 1.

We can see from Table 1 that the errors in the angles are quite large for vertical tracks. The primary reason is that the current generation of Timepix detectors has a pixel size of 55 μm and a 300 μm thick Si sensor layer, which makes it difficult to distinguish a 0 degree incidence and a 15 degree incidence. We hope an improvement will be made with the next generation, which may have a smaller-sized pixels. However, in an isotropic flux of incident particles, the solid angle acceptance for vertical tracks is small, so the relative numbers will not be large. In addition, an estimate of the track length is

relatively insensitive to the error in the angle for angles of incidence near vertical, and is less than or on the order of the stochastic variation in the energy loss of the primary ions. So the errors on vertical track angle determination can be tolerated in determining the dose equivalent at this point.

Table 1 also shows the LET estimation using angular resolutions above, combined with total energy deposited from energy calibration method. In this table, we expect the LET values of the same source of particles to have the same value for different angles. However, due to plasma-effect [6], which comes from the recombination of high densities of electrons and holes, the estimate of the amount of energy deposited is reduced. This effect occurs to the greatest extent in the regions of greatest ion density in the sensor, and where the bias voltage field direction is parallel to the track direction. This is the most likely explanation for different values of LETs for different angles of the same source of particles. We are in the process of studying this effect, and will try to develop an algorithm to compensate for this loss in future work.

Table 1. Angle and LET resolution

	0		20		30		40		45		60		75		85	
	Angle	LET	Angle	LET	Angle	LET	Angle	LET	Angle	LET	Angle	LET	Angle	LET	Angle	LET
H-160	**10.5**	1			**28.6**	1			**42.6**	1	**57**	1				
He-100	**15.5**	4.8			**32.8**	5					**60**	5	**74.2**	5.2		
He-180					**32.7**	1			**46.4**	1	**60.7**	1				
C-230	**9**	17.3			**26.1**	17.9			**43.6**	16	**60.8**	13.9			**86**	13.7
N-290	**6.4**	41.1			**30.8**	40.9					**60.2**	36.1	**75.1**	33.6		
O-230	**9.3**	62.7	**24.3**	64.2			**40.5**	71.5			**61.2**	40.3			**85**	70.5
Ne-600	**9.3**	61.3	**24.2**	61.7			**40.2**	72.2			**60.3**	70.4			**85**	63.7
Ar-290	**9.7**	100.4			**30.4**	105.5					**59.5**	118.6			**85**	139.3
Ar-650	**7.4**	82			**29.2**	95.5					**59.4**	97.1			**85**	115.9
Fe-400	**7.6**	196.3			**27.2**	215.8					**59.4**	242.1	**75.9**	256.4		

5. Future work

Future work will automate the detailed classification of the incident ionizing radiation in a typical space mission exposure using a machine learning approach. We plan to extract relevant features from the track and use a classifier to recognize the properties of the incident particle. In addition to LET, δ-rays and distributions of energy deposited are taken into account to get information about velocity, which is an important factor for classification resolution [5].

References

[1] Holy T, Heijne E, Jakubek J, Pospisil S, Uher J and Vykydal Z 2008 Pattern recognition of tracks induced by individual quanta of ionzining radiation in Medipix2 silicon detector. *Nucl. Instr. and Meth.* A **598** 287-290

[2] Bouchami J, Gutierrez A, Houdayer A, Jakubek J, Lebel C, Leroy C, Macana J, Martin P, Platkevic M, Pospısil S and Teyssier C 2011 Study of the charge sharing in silicon pixel detector by means of heavy ionizing particles interacting with a Medipix2 device. *Nucl. Instr. and Meth.* A **633** 117-120

[3] Kroupa M, Jakubek J and Krejci F 2008 Charge Collection Characterization with Semiconductor Pixel Detector Timepix. *IEEE Nucl. Science Symposium Conf. Record*

[4] Jakubek J 2011 Precise Energy Calibration of Pixel Detector Working in Time-Over-Threshold

Mode. *Nucl. Instr. and Meth.* A **633** 262-266
[5] Pinsky L, Empl A, Gutierrez A, Jakubek J, Kitamura H, Miller J, Leroy C, Stoffle N, Pospisil S, Uchihori Y, Yasuda N and Zeitlin C 2011 Penetrating heavy ion charge and velocity discrimination with a TimePix-based Si detector (for space radiation applications). *Nucl. Instr. and Meth.* A **633** 190-193
[6] Williams R and Lawson E 1974 The plasma effect in silicon semiconductor radiation detectors. *Nucl. Instr. and Meth.* **120** 261-268
[7] Zadeh L 1965 Fuzzy sets. *Information and Control* **8** 338–353